Numerical Simulations of Imploding Detonations

Lisong Shi, Chih-Yung Wen
Department of Aeronautical and Aviation Engineering
The Hong Kong Polytechnic University
Hong Kong

1 Introduction

The inward-symmetrically propagating cylindrical detonation waves can generate extreme thermal states upon reaching the singularity at the center of the collapse. Notable early research on imploding detonations includes several influential studies by Knystautas & Lee [1,2] and Ahlborn & Huni [3]. The curvature distribution mechanism was suggested to smooth out the corrugated front [2]. Oran & DeVore [5] numerically studied cylindrically imploding detonation and quantitative agreement was found compared to the Chester-Chisnell-Whitham theory. More recently, Rodriguez Rosero et al. [4] has revisited this topic through a series of high-quality experiments, exploring the mechanisms responsible for asymmetric implosion. To better understand the implosion from a numerical perspective, this paper focuses on simulating the two-dimensional polygonal detonation implosion process.

2 Physical modelling

As an initial attempt at numerically simulating detonation implosion, the impact of the initial ignition process on the final results remains unclear. Additionally, using detailed chemical models is computationally expensive, as the simulation domain can easily span thousands of detonation cells. Such high-cost computations may be feasible once the general behavior of numerical detonation implosion is more thoroughly understood. Therefore, this study employs a simplified reaction model, specifically the non-dimensional Euler equations with a one-step chemical model. This model has been widely applied in the study of large-scale multi-dimensional detonation simulations such as diverging detonations [6] and three-dimensional detonation structures [7]. We follow the governing equations in [6, 7] that employ the non-dimensional forms, one-step reaction model, and neglect viscous effects. The chemical reaction rate follows the Arrhenius equation $\dot{\omega} = -K\rho\lambda e^{-\frac{E_a}{T}}$, where E_a is the activation energy set to 27 in the present simulations, and K is a scaling factor adjusted to ensure that the half-reaction length (δ) in the ZND profile is of unit length scale. The other parameters selected are $\gamma = 1.2$ and $Q = 50$. Here, small hot spots are arranged to form a line of ignition sources, with several such lines collectively creating the initial polygonal detonation. The schematic of the example hexagonal implosion is described in Fig. 1. The reactive gas is surrounded by hexagonal ignition sources (with $n = 6$ edges), and the inert gas lies outside. The distance from the center to the edge of ignition source, denoted as *r*, is kept constant at 700

Correspondence to: C. Y. Wen, cywen@polyu.edu.hk

unit lengths for all cases in the present study. The present simulations are performed using adaptive mesh refinement with the finest level of resolution set to 10 pts/δ.

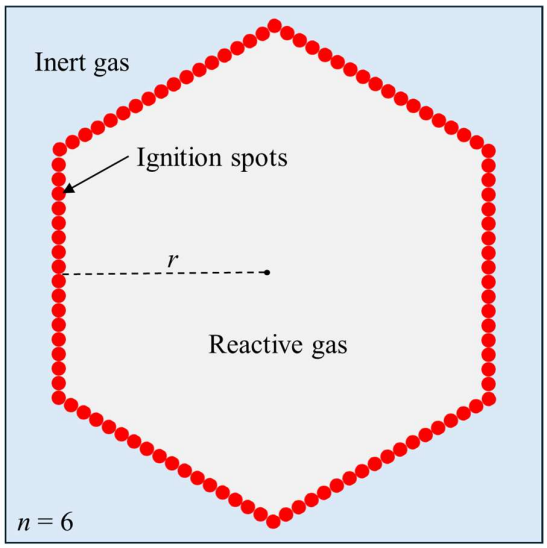

Figure 1. Schematic of the simulation setup for imploding detonation.

3 Numerical results

We present simulation results for n = 3, 6, 18, and ∞, respectively. Figure 2 shows the density fields at two timesteps approaching the final collapse for $n = 3$. Each ignition line forms a cellular detonation wavefront, with the initial small cells resulting from initial perturbations. These small cells quickly transition to weakly irregular structures. The dark region near the center results from the detonation reflection at the point of focus. The angle between a neighboring detonation front and the plane of symmetry formed by two adjacent detonation surfaces is sufficiently small to ensure regular detonation reflection. As a result, the ignition shape essentially remains unchanged until near the center, where the size of the unreacted region becomes comparable to the cellular structure. This consistency in the detonation fronts is also observed in Figure 2d.

Figure 3 presents results for cases with more ignition lines or a circular ignition source. When the number of edges is increased to $n = 6$, Mach reflections of cellular detonation [8] occur, and the fronts transform into a roughly irregular dodecagon and the secondary reflections occur at around $t = 80$. The average cell size swept by the Mach stem decreases due to local overdriving. Further increasing the number of edges to $n = 18$ results in a larger angle for the triple-point trajectory. As a result, the detonation fronts soon become indistinguishable from circular. Two families of logarithmic spirals are recorded on these soot foils. Towards the center, transverse merging is observed, and the cell size also decreases.

The detonation front locations (from one ignition line to the center) as a function of time for all cases are summarized in Figure 4, along with the CJ slope. The $n = 3$ case closely follows the CJ slope, as it exhibits regular reflection. The $n = 6$ case deviates from the CJ slope starting around $t = 80$, when the secondary reflections occur. The case with a circular ignition source accelerates from the beginning, and the $n = 18$ case follows a similar trajectory. The acceleration of the detonation front is expected to be even more pronounced as $r \to 0$. Since velocity is a higher-order derivative of front location, and given

the presence of cellular instability and possible numerical limitations, accurately determining the final stage near the center is challenging. Further detailed analysis is currently underway.

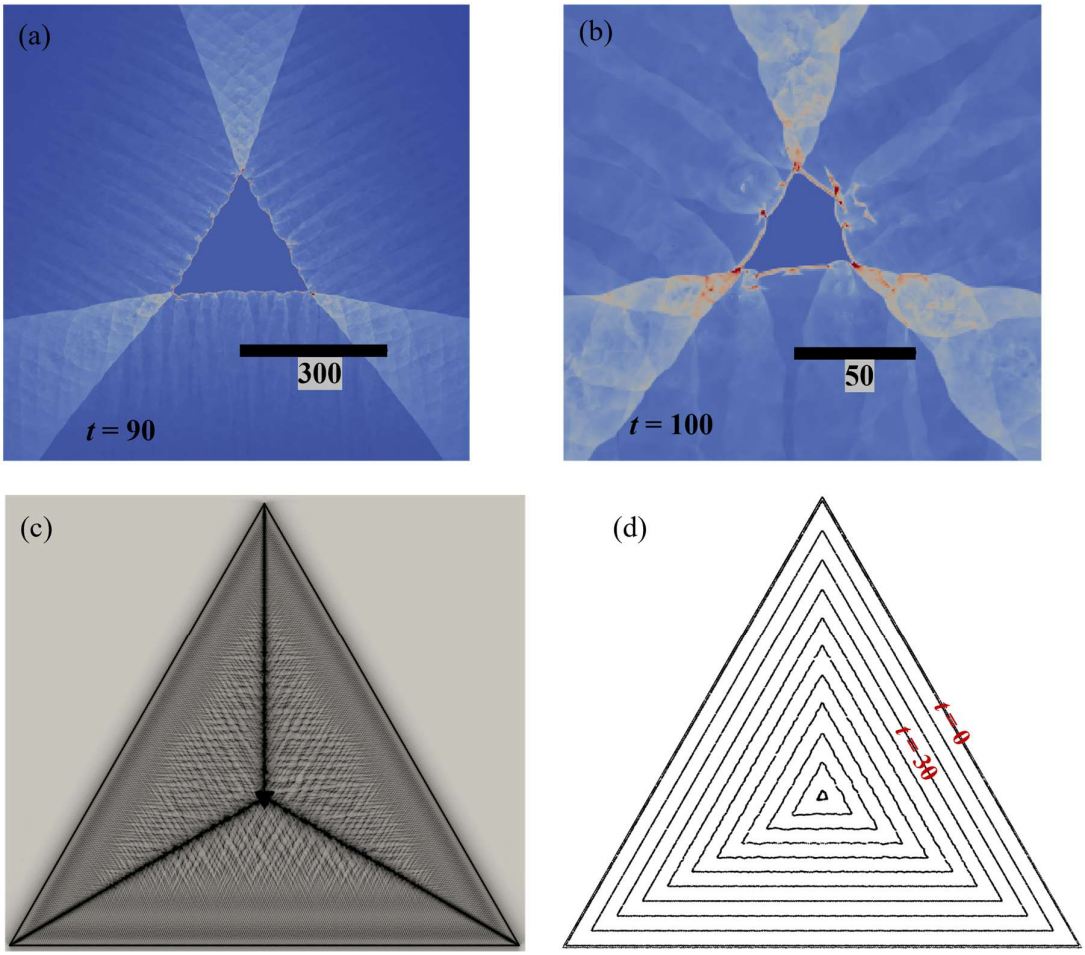

Figure 2. Implosion with $n = 3$. (a, b) Density contours; (c) Soot foil; (d) Detonation fronts with a time interval of 10.

4 Concluding remarks

In this study, a sufficiently large distance of travel for the imploding detonation was computed. The results showed both regular and Mach reflection of cellular detonations during implosion. In the case of regular type of reflection, the detonation front profiles remained consistent, with no acceleration observed. In contrast, the combination of Mach reflection and cellular instability facilitated the transition to a more circular shape. Further results and a detailed analysis will be presented during the conference.

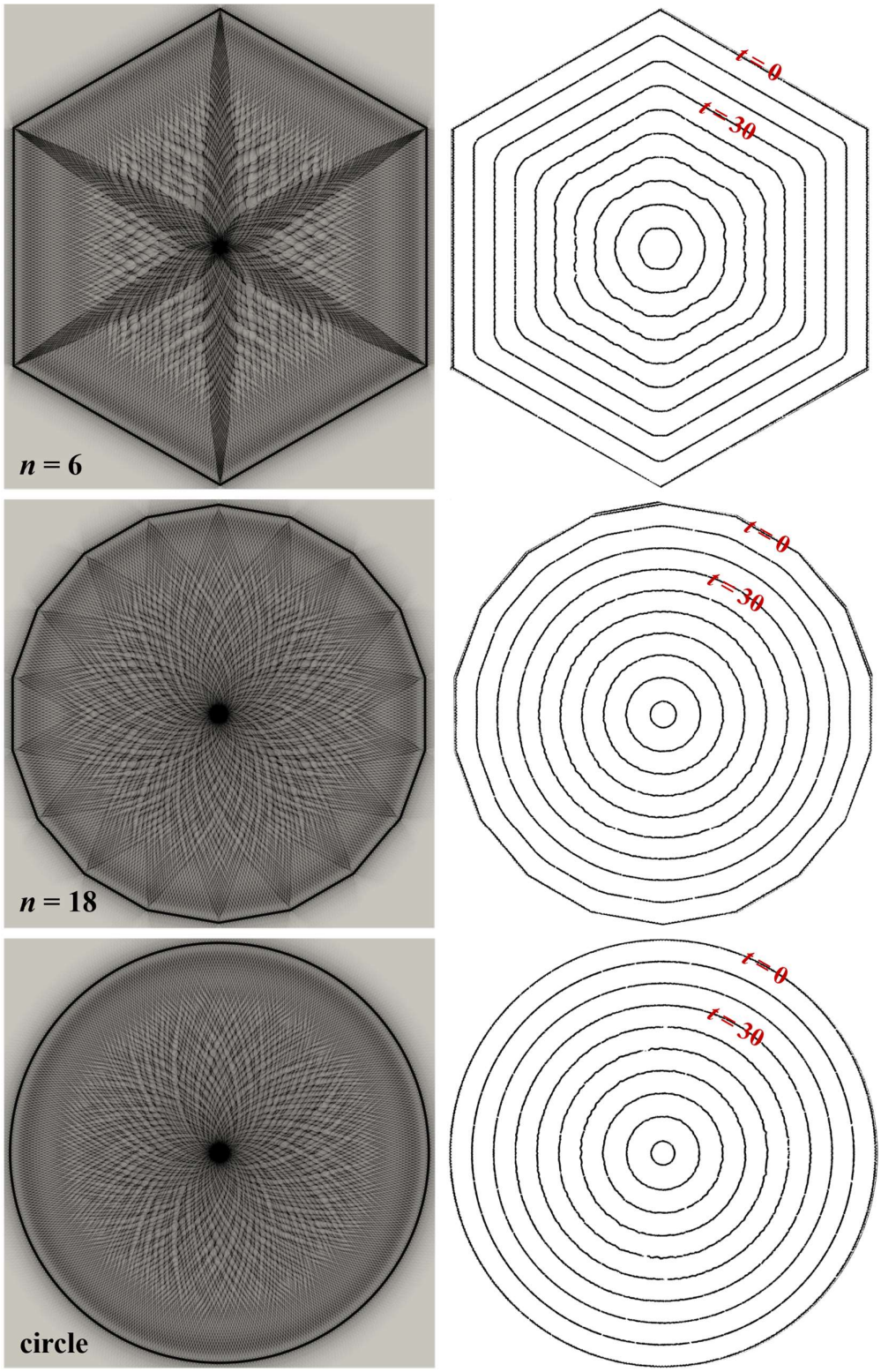

Firgure 3. Soot foils and wave fronts with time interval of 10.

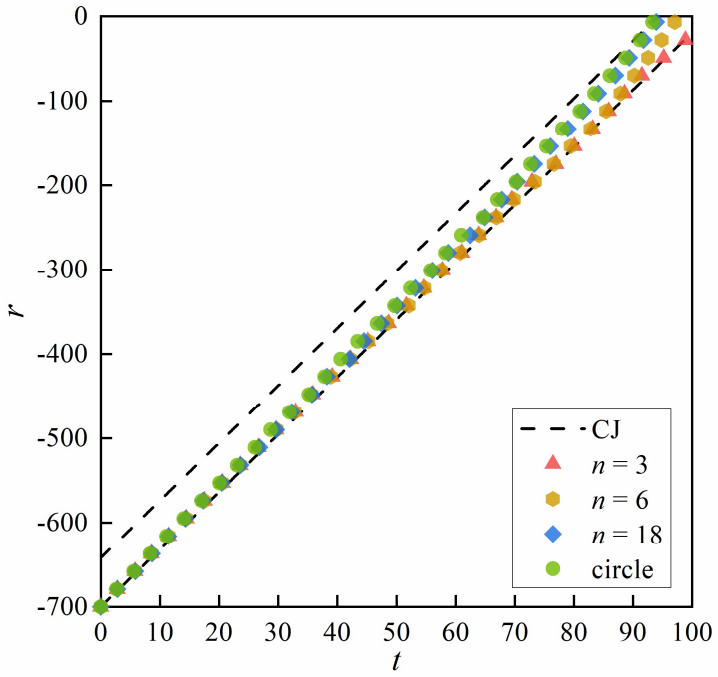

Figure 4. Detonation fonts location.

References

[1] Knystautas, R., Lee, J. H. (1967). Spark initiation of converging detonation waves. AIAA Journal, 5(6), 1209-1211.

[2] Knystautas, R., Lee, J. H. (1971). Experiments on the stability of converging cylindrical detonations. Combustion and Flame, 16(1), 61-73.

[3] Ahlborn, B., Huni, J. P. (1969). Stability and space-time measurements of concentric detonations. AIAA Journal, 7(6), 1191-1192.

[4] Rodriguez Rosero, S., Loiseau, J., Higgins, A. J. (2024). Asymmetry of imploding detonations in thin channels. Shock Waves, 34(5), 413-427.

[5] Oran, E. S., DeVore, C. R. (1994). The stability of imploding detonations: Results of numerical simulations. Physics of Fluids, 6(1), 369-380.

[6] Shen, H., Parsani, M. (2017). The role of multidimensional instabilities in direct initiation of gaseous detonations in free space. Journal of Fluid Mechanics, 813, R4.

[7] Shi, L., Wen, C. Y., Sun, X., Fan, E. (2024). Detonation propagation in three-dimensional continuous curved ducts. arXiv preprint:2409.19944.

[8] Li, J., Lee, J. H. (2016). Numerical simulation of Mach reflection of cellular detonations. Shock Waves, 26(5), 673-682.